

Investigation of Enzyme Kinetics Using Quench–Flow Techniques with MALDI-TOF Mass Spectrometry

Christopher T. Houston,[†] William P. Taylor,[‡] Theodore S. Widlanski, and James P. Reilly*

Department of Chemistry, Indiana University, Bloomington, Indiana 47405

Matrix-assisted laser desorption/ionization time-of-flight (MALDI-TOF) mass spectrometry is combined off-line with rapid chemical quench–flow methods to investigate the pre-steady-state kinetics of a protein-tyrosine phosphatase (PTPase). PTPase kinetics are generally interrogated spectrophotometrically by the employment of an artificial, chromophoric substrate. However, that methodology places a constraint on the experiment, hampering studies of natural, biochemically relevant substrates that do not incorporate a chromophore. The mass spectrometric assay reported herein is based on the formation of a covalent phosphoenzyme intermediate during substrate turnover. This species is generated in the reaction regardless of the substrate studied and has a molecular weight 80 Da greater than that of the native enzyme. By following the appearance of this intermediate in a time-resolved manner, we can successfully measure pre-steady-state kinetics, regardless of the incorporation of a chromophore. The strengths of the mass-spectrometric assay are its uniform response to all substrates, simple and direct detection of covalent enzyme–substrate intermediates, and facile identification of enzyme heterogeneities that may affect enzymatic activity.

In the field of enzyme kinetics, spectrophotometric methods are used extensively to monitor product formation during catalysis.¹ This requires artificial substrates that undergo a color change upon turnover. Thus, as the reaction proceeds, an increase in absorbance at a given wavelength is produced. Although this is a simple and effective means for kinetic analysis, the scope of substrates that can be studied is highly restricted. Furthermore, natural substrates for the enzyme generally cannot be assayed in this manner. A different type of detector that responds universally to all substrates would have definite advantages over the spectrophotometric system.

Within the past decade, analysis of biological systems by matrix-assisted laser desorption/ionization time-of-flight (MALDI-TOF) mass spectrometry has evolved from the novel to the

routine. Although MALDI-TOF is regularly used to study the products of enzyme reactions, few authors have employed it to probe the actual course of enzymatic reactions. Examples in the literature of kinetic analyses by MALDI-TOF generally involve rather simple steady-state measurements. For example, time-course studies of peptide phosphorylation and dephosphorylation have been demonstrated by Craig et al.² and Matsumoto et al.³ Gonnet et al. used a combination of electrospray ionization mass spectrometry and MALDI-TOF to determine the rate at which cisplatin binds with single-stranded DNA oligomers.⁴ Although steady-state measurements can extract Michaelis constants (K_m) and turnover numbers (k_{cat}), little to no direct information about individual steps along the catalytic pathway can be revealed in this manner. However, this type of detailed information can be derived from pre-steady-state measurements. Despite this fact, the realm of pre-steady-state kinetic measurements by MALDI-TOF remains unexplored.

Enzyme kinetics have been studied in somewhat greater detail using electrospray ionization (ESI) mass spectrometry. Early applications were relatively simple. Ashton and co-workers used ESI to demonstrate that the serine proteases, α -chymotrypsin, subtilisin Carlsberg, and subtilisin BPN, turn substrate over through a covalent O-acyl intermediate.⁵ Nairn used ESI mass spectrometry to measure half-lives for the dephosphorylation of two phosphoglycerate mutases under various conditions.⁶ In a more complex study, Saves et al. examined the effects of a point mutation on the activity of β -lactamase TEM-1 with various β -lactam antibiotics.⁷

Recently, Northrup and Simpson suggested that coupling quench–flow methods with mass spectrometry has the potential to reveal kinetic information about enzymes that is difficult or impossible to extract using conventional spectrophotometric analyses.¹ By replacing a spectrophotometer with a mass spectrometer, the analyst gains the ability to observe the progress of

* Corresponding Author: James P. Reilly. Phone: (812) 855–1980. Fax: (812) 855-8300. email: reilly@indiana.edu.

[†] Current address: Pharmacia & Upjohn, 7234-259-277, 7000 Portage Rd., Kalamazoo, Michigan 49001-0199.

[‡] Current address: College of Pharmacy, University of Michigan, 428 Church St., Ann Arbor, Michigan 48109-1065.

(1) Northrup, D. B.; Simpson, F. B. *Bioorg. Med. Chem.* **1997**, *5*, 641–644.

(2) Craig, A. G.; Hoeger, C. A.; Miller, C. L.; Goedkin, T.; Rivier, J. E.; Fischer, W. H. *Biol. Mass Spectrom.* **1994**, *23*, 519–528.

(3) Matsumoto, H.; Kahn, E. S.; Komori, N. *Anal. Biochem.* **1998**, *260*, 188–194.

(4) Gonnet, F.; Kochler, F.; Blais, J. C.; Bolbach, G.; Tabet, J. C.; Chottard, J. C. *J. Mass Spectrom.* **1996**, *31*, 802–809.

(5) Ashton, D. S.; Beddell, C. R.; Cooper, D. J.; Green, B. N.; Oliver, R. W. A.; Welham, K. J. *FEBS Lett.* **1991**, *292*, 201–204.

(6) Nairn, J.; Krell, T.; Coggins, J. R.; Pitt, A. R.; Fothergill-Gilmore, L. A.; Walter, R.; Price, N. C. *FEBS Lett.* **1995**, *359*, 192–194.

(7) Saves, I.; Burlet-Schiltz, O.; Maveyraud, L.; Samama, J.-P.; Promé, J.-C.; Masson, J.-M. *Biochemistry* **1995**, *34*, 11660–11667.

enzyme turnover, regardless of the incorporation or lack of a chromophore in the substrate.¹ The mating of quench–flow devices with mass spectrometry should improve the temporal resolution of kinetic measurements from tens of seconds to a few milliseconds.

Paiva et al. coupled rapid mixing instrumentation on-line with an ESI mass spectrometer.⁸ Reactions were quenched upon desolvation in the ESI source. This allowed the authors to trap and detect the low molecular weight (<500 Da) intermediates formed when shikimate-3-phosphate and phosphoenol pyruvate are converted to 5-enolpyruvoyl-shikimate-3-phosphate (EPSP) and inorganic phosphate by the enzyme EPSP synthase. No time-course data were presented, although the potential to extract kinetic information was clearly evident.⁸

The first combination of biological mass spectrometry with quench–flow methods for the purpose of measuring pre-steady-state kinetics was accomplished by Zechel et al. using an ESI instrument.⁹ As a model system, they studied a mutation of *Bacillus circulans* xylanase. Their home-built quench–flow apparatus allowed them to observe the appearance of a covalent enzyme–substrate intermediate with temporal resolution on the order of tens of milliseconds.

This account describes the first coupling of rapid quench–flow methods with MALDI-TOFMS to measure pre-steady-state kinetics. The subject of this investigation is the low molecular weight phosphatase Stp1 ($m/z = 17\,390.8$ Da), isolated from *Schizosaccharomyces pombe*. Stp1 catalyzes the dephosphorylation of both phosphotyrosine and phosphothreonine substrates. However, it is more active toward aryl phosphates and thus behaves more like a protein tyrosine phosphatase (PTPase).¹⁰ This yeast phosphatase shares a great deal of sequence and activity homology with its human counterparts.¹¹ In fact, it can function in place of Cdc25, an essential PTPase in the mammalian cell cycle.^{11,12}

PTPases convert phosphotyrosine to tyrosine via the mechanism depicted in Figure 1.¹³ All PTPases contain a conserved cysteine residue in the active site that becomes a nucleophilic thiolate when deprotonated. After substrate binding, the thiolate makes a nucleophilic attack on the phosphorus atom of the phosphate and displaces a phenoxide leaving group. In Stp1, Asp128 protonates the leaving group to generate a phenol.¹⁴ During this step, the enzyme forms a covalent phosphoenzyme (EP) intermediate. The key to mass-spectrometric analysis of PTPases lies in the +80 Da mass shift of EP relative to unphosphorylated enzyme. In the final step of the mechanism, EP is hydrolyzed to regenerate the enzyme catalyst and release inorganic phosphate.

Spectrophotometric assays of PTPases generally use *p*-nitrophenyl phosphate (*p*-NPP) as an artificial substrate. Under our conditions, nonhydrolyzed *p*-NPP has an extinction coefficient of

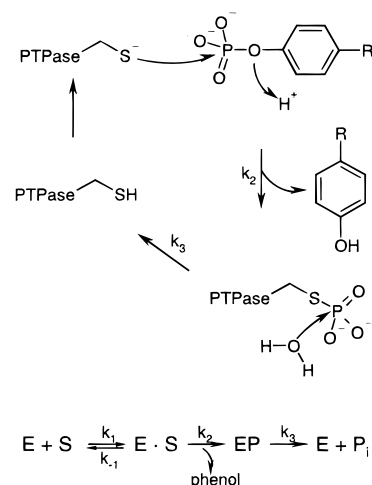


Figure 1. Mechanism employed by protein tyrosine phosphatases (PTPases) to catalyze the hydrolysis of aryl phosphate esters. To detect the phosphoenzyme (EP) intermediate by mass spectrometry, k_2 must be faster than k_3 .

$40\text{ M}^{-1}\text{ cm}^{-1}$ at 400 nm. Upon release of the phenoxide product (Figure 1), ϵ increases to $18\,000\text{ M}^{-1}\text{ cm}^{-1}$. Given that all substrates are turned over through an EP intermediate, mass spectrometry appears to be an attractive substrate-independent method for PTPase analysis. For any given PTPase, the same EP chemical moiety is generated from all substrates. Consequently, we expect the mass spectrometer to respond uniformly to EP regardless of substrate, and so the use of chromophoric substrates such as *p*-NPP becomes unnecessary. To make these types of measurements, the mass spectrometer resolving power must be sufficient to distinguish unphosphorylated enzyme from EP. Furthermore, formation of EP must proceed more rapidly than hydrolysis ($k_2 > k_3$). Otherwise, EP does not accumulate to a detectable concentration in solution.

Quantitation of EP from the mass spectrum is the most important issue at the heart of this analysis. In general, MALDI is considered a qualitative, not a quantitative, technique. Sample preparations tend to be inhomogeneous, leading to variability in ion signal intensity on a shot-to-shot and sample-to-sample basis. Furthermore, the presence of certain sample components such as buffers, salts, or other proteins can enhance or suppress analyte ion signal intensity. Despite the shortcomings of current MALDI protocols, several authors have demonstrated that quantitation is possible.^{15–30}

- (8) Paiva, A. A.; Tilton, R. F.; Crooks, G. P.; Huang, L. Q.; Anderson, K. A. *Biochemistry* **1997**, *36*, 15472–15476.
 (9) Zechel, D. L.; Konermann, L.; Withers, S. G.; Douglas, D. J. *Biochemistry* **1998**, *37*, 7664–7669.
 (10) Zhang, Z.-Y.; Zhou, G.; Denu, J. M.; Wu, L.; Tang, X.; Mondesert, O.; Russell, P.; Butch, E.; Guan, K.-L. *Biochemistry* **1995**, *34*, 10560–10568.
 (11) Mondesert, O.; Moreno, S.; Russell, P. *J. Biol. Chem.* **1994**, *269*, 27996–27999.
 (12) Weinert, T. *Science (Washington, D.C.)* **1997**, *277*, 1450–1451.
 (13) Widlanski, T. S.; Taylor, W. P. In *Comprehensive Natural Products Chemistry*, Vol. 5; Poulter, C. D., Ed.; Elsevier: New York, 1999; pp 139–162.
 (14) Wu, L.; Zhang, Z.-Y. *Biochemistry* **1996**, *35*, 5426–5434.

- (15) Nicola, A. J.; Gusev, A. I.; Hercules, D. M. *Appl. Spectrosc.* **1996**, *50*, 1479–1482.
 (16) Nelson, R. W.; McLean, M. A.; Hutchens, T. W. *Anal. Chem.* **1994**, *66*, 1408–1415.
 (17) Ammon, D.; Soltys, C.; Valint, P.; Grobe, G.; Gardella, J.; Wood, T. Proceedings of the 47th ASMS Conference on Mass Spectrometry and Ion Processes, Dallas, Texas, June 13–17, 1999.
 (18) Gusev, A. I.; Wilkinson, W. R.; Proctor, A.; Hercules, D. M. *Fresenius' J. Anal. Chem.* **1996**, *354*, 455–463.
 (19) Muddiman, D. C.; Gusev, A. I.; Proctor, A.; Hercules, D. M. *Anal. Chem.* **1994**, *66*, 2362–2368.
 (20) Jespersen, S.; Niessen, W. M. A.; Tjaden, U. R.; van der Greef, J. *J. Mass Spectrom.* **1995**, *30*, 357–364.
 (21) Hensel, R. R.; King, R. C.; Owens, K. G. *Rapid Commun. Mass Spectrom.* **1997**, *11*, 1785–1793.
 (22) Preston, L. M.; Murray, K. K.; Russell, D. H. *Biol. Mass Spectrom.* **1993**, *22*, 544–550.
 (23) Vorm, O.; Roepstorff, P.; Mann, M. *Anal. Chem.* **1994**, *66*, 3281–3287.

Internal standards are often used to compensate for variations in sample preparation or shot-to-shot laser intensity. Ideally, they should be desorbed and ionized during MALDI with an efficiency similar to that of the analyte. Furthermore, they should be resolvable in mass from the analyte. Although isotopically labeled internal standards work well for molecules smaller than 500 Da,¹⁵ the resolving power of MALDI-TOF is not sufficient for this approach to be feasible with proteins. Nelson et al. employed myoglobin as an internal standard for cytochrome *c*.¹⁶ They were able to calculate molar response factors for each binary system to predict how the signal of the internal standard varies with analyte concentration. A more systematic extension of this idea was recently presented by Ammon et al.¹⁷

Choice of the internal standard should be made judiciously. For example, using an internal standard that is a structural analogue of the analyte increases the likelihood that both species will be incorporated into the dried matrix crystal in a similar manner. This approach has been used by Hercules' group to carry out numerous quantitative MALDI experiments on cyclosporin A with cyclosporin D as an internal standard.^{18,19} Jespersen et al. used bovine cytochrome *c* as an internal standard for equine cytochrome *c* because they differ only by three amino acids.²⁰ Bovine cytochrome *c* contains one fewer lysine residue than equine, however, and the authors concluded that a protein with similar proton affinity might have been a better choice for the internal standard.

In addition to the use of internal standards, other avenues have been explored to improve the quantitation of MALDI experiments. For example, some authors have sought to improve the absolute reproducibility of ion signals. Use of electrospray sample deposition,²¹ nitrocellulose substrates,²² fast matrix evaporation,^{23,24} and matrix additives^{25,26} has yielded a more consistent ion signal across MALDI sample preparations when compared with the conventional "dried-droplet" approach. In some cases, researchers have focused on data processing methods to improve the quantitative data obtained from MALDI experiments.^{27–29} These techniques include mathematical deconvolution of overlapping Gaussians²⁸ and employment of parabolic or spline-shaped nonlinear baseline subtractions.²⁹

For our kinetic analysis of Stp1, unphosphorylated Stp1 acts as an ideal internal standard for EP. Although some authors have noted an ionization bias against phosphorylated peptides relative to their unphosphorylated analogues,² this observation was made for peptides containing 7 to 14 amino acid residues. We assume that attachment of phosphate to a protein as large as Stp1 (156 amino acids, $m/z = 17\,390.8$ Da) does not perturb its ionization

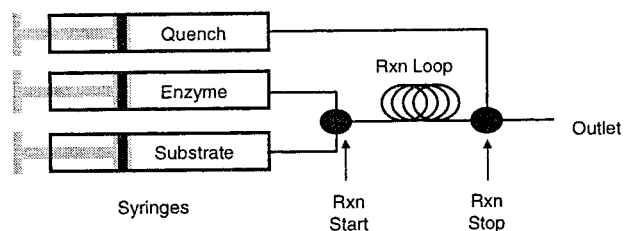


Figure 2. Block diagram of quench flow apparatus.

efficiency notably. The validity of this assumption is addressed later in this work.

This paper describes our development of a pre-steady-state kinetics assay comprised of a quench–flow instrument coupled off-line with MALDI-TOF mass spectrometry. Important issues in the creation of this assay include the ability to trap and detect EP and reliable quantitation of EP relative to unphosphorylated enzyme. A comparison of data obtained from MALDI-TOF and spectrophotometric assays is presented. Finally, we examine a series of nonchromophoric substrates and demonstrate that the quench–flow MALDI technique can measure the effects of substrate variation on catalysis.

EXPERIMENTAL SECTION

Materials. Preliminary samples of Stp1 and a plasmid encoding this protein were kindly provided by Zhong-Yin Zhang from the Albert Einstein College of Medicine. Ferulic acid and dichloroacetic acid were obtained from Aldrich (Milwaukee, WI). Dichloroacetic acid was freshly distilled under reduced pressure before use. TPCK-trypsin, equine myoglobin, *p*-nitrophenyl phosphate, CM Sephadex C-50-120, Sephadex G-100-200, Sephadex G-25-50, and α -cyano-4-hydroxycinnamic acid were purchased from Sigma (St. Louis, MO). Trifluoroacetic acid (TFA) was obtained from EM Science (Gibbstown, NJ). 3,3-Dimethylglutaric acid was purchased from Fluka and recrystallized from ethyl acetate/hexanes prior to use. The dicyclohexylammonium salts of *p*-fluorophenyl phosphate (*p*-FPP), *p*-methylphenyl phosphate (*p*-MePP), phenyl phosphate (PP), 3,4-dimethylphenyl phosphate (3,4-DMPP), and trifluoroethyl phosphate were synthesized by Stephen Antonelli (Indiana University, Bloomington, IN).

Steady-State Trapping Experiments. Our original enzyme stock solution (provided by Z.-Y. Zhang) contained 390 μ M Stp1 buffered in 100 mM sodium acetate, 100 mM sodium chloride, and 1 mM EDTA (pH 5.1).⁷ Phosphoenzyme (EP) intermediates were trapped in the steady state by mixing 1 μ L of Stp1 stock with 28.3 μ L of 15 mM ammonium acetate buffer (pH 5) containing 300 μ M *p*-nitrophenyl phosphate (*p*-NPP). The reaction was quenched within three seconds by adding 12.2 μ L of ferulic acid solution and vortexing. Ferulic acid (32.5 mg/mL) was dissolved in absolute ethanol containing 1% TFA (v/v). The final concentration of enzyme was approximately 9.5 μ M. Two microliters of this mixture were deposited directly onto the stainless steel MALDI probe for mass analysis.

Pre-Steady-State Analysis. Quench–flow experiments were accomplished using an RQF-3 rapid chemical quench–flow instrument (KinTek Corporation, Austin, TX). As shown in Figure 2, this instrument consists of three syringes driven by a stepper motor. These syringes contain substrate, enzyme, and quench solutions. Reaction is initiated upon mixing of enzyme and

(24) Nicola, A. J.; Gusev, A. I.; Proctor, A.; Jackson, E. K.; Hercules, D. M. *Rapid Commun. Mass Spectrom.* **1995**, *9*, 1164–1171.

(25) Gusev, A. I.; Wilkinson, W. R.; Proctor, A.; Hercules, D. M. *Anal. Chem.* **1995**, *67*, 1034–1041.

(26) Gusev, A. I.; Muddiman, D. C.; Proctor, A.; Sharkey, A. G.; Hercules, D. M.; Tata, P. N. V.; Venkataramanan, R. *Rapid Commun. Mass Spectrom.* **1996**, *10*, 1215–1218.

(27) Muddiman, D. C.; Gusev, A. I.; Stoppek-Langner, K.; Proctor, A.; Hercules, D. M.; Tata, P. N. V.; Venkataramanan, R.; Diven, W. *J. Mass Spectrom.* **1995**, *30*, 1469–1479.

(28) Tang, X.; Sadeghi, M.; Olumee, Z.; Vertes, A.; Braatz, J. A.; McLain, L. K.; Dreifuss, P. A. *Anal. Chem.* **1996**, *68*, 3740–3745.

(29) Wilkinson, W. R.; Gusev, A. I.; Proctor, A.; Houalla, M.; Hercules, D. M. *Fresenius' J. Anal. Chem.* **1997**, *357*, 241–248.

(30) Muddiman, D. C.; Gusev, A. I.; Hercules, D. M. *Mass Spectrom. Rev.* **1995**, *14*, 383–429.

substrate. The reaction progresses as the mixture is pumped through a variable-length reaction loop. After the reaction loop, a quench solution is infused into the mixture which halts the reaction. Reaction times from 4 ms to 1 s were studied by varying reaction loop length and flow rate through the instrument. The device was temperature-controlled at 20 °C.

To ensure the availability of fresh enzyme, all pre-steady-state experiments were performed with Stp1 expressed in-house and purified as previously reported.¹⁰ Following size exclusion chromatography, the protein was buffer-exchanged on a Sephadex G-25 Superfine column (1.5 cm × 8 cm) equilibrated in 25 mM ammonium 3,3-dimethylglutarate, 50 mM ammonium chloride, and 1 mM EDTA at pH 6.5 (DMG buffer). Active fractions were pooled, concentrated, passed through a 0.2- μ m sterile membrane filter, and stored at 4 °C until use. Enzymatic activity remained unchanged over several months under these conditions.

Steady-state enzymatic activity was determined in DMG buffer at 20 °C by quantitating the release of inorganic phosphate from the phosphate esters using the Lanzetta assay.³¹ The steady-state parameters K_m and V_{max} were determined from a linear replot of substrate concentration and velocity data pairs ($[S]/v$ against v). Substrate concentrations ranged from 0.25 K_m to 5 K_m . The value of k_{cat} was determined from V_{max} and enzyme concentration in the reaction mixture. K_m and k_{cat} were also determined for *p*-NPP by quantitation of *p*-nitrophenoxide release ($\epsilon = 18\,000\text{ M}^{-1}\text{ cm}^{-1}$ at 400 nm) and were identical to determinations made by inorganic phosphate release.

Enzyme stock solutions contained 120 μ M Stp1, as determined using a BCA Protein Assay Kit (Pierce no. 23226T). Substrate was dissolved at various concentrations in the same buffer. Reactions were quenched by mixing 0.5 M aqueous dichloroacetic acid into the mixture. Although TFA works well as a quench for trapping experiments in acetate buffer, use of TFA in the DMG buffer system results in protein precipitation. This is problematic, as it leads to light scattering in the spectrophotometer and highly inconsistent MALDI sample preparations. The switch to dichloroacetic acid for quenching eliminates protein precipitation problems. Each experiment consumed 13.9 μ L of Stp1, 14.9 μ L of substrate, and 143.4 μ L of quench. Thirty-eight microliters of additional DMG buffer were used to flush the reaction products out of the quench–flow apparatus. Stp1 concentration was 10 μ M in the final quenched volume prior to MALDI-TOF analysis.

Spectrophotometric Studies. To check the validity of the MALDI-TOF assay, spectrophotometric analysis of pre-steady-state kinetics was performed in-parallel, using *p*-NPP as substrate. At 400 nm, we determined that *p*-nitrophenoxide absorbs strongly with $\epsilon = 18\,000\text{ M}^{-1}\text{ cm}^{-1}$. To ensure that the product phenol was fully deprotonated, 50 μ L of 5 M NaOH in 10% (v/v) ethanol and 100 μ L of chloroform were added to the quenched reaction mixture. Ethanol and chloroform serve to reduce foaming in the mixture for more reliable spectrophotometric readings. Absorbance measurements were made on a Shimadzu UV160U spectrophotometer.

Absorbance data were converted to concentration of nitrophenol, plotted as a function of time, and fit to eq 1.

$$[p\text{-nitrophenol}] = At + B(1 - e^{-bt}) \quad (1)$$

A , B , and b are constants described by eqs 2, 3, and 4.

$$A = \frac{[E]_0[S]_0 \frac{k_2 k_3}{(k_2 + k_3)}}{[S]_0 + K_m} \quad (2)$$

$$B = \frac{\left(\frac{k_2}{k_2 + k_3}\right)^2 [E]_0}{\left(1 + \frac{K_m}{[S]_0}\right)^2} \quad (3)$$

$$b = k_3 + \frac{k_2}{1 + [(k_2 + k_3)K_m/k_3[S]_0]} \quad (4)$$

Here, time (t) is in seconds, K_m is the Michaelis constant, $[S]_0$ denotes the initial substrate concentration, and $[E]_0$ is the initial enzyme concentration in the reaction mixture. The derivation of these equations is based on that published by Bender et al.³²

Matrix-Assisted Laser Desorption/Ionization Time-of-Flight Mass Spectrometry. Several matrixes were tested for Stp1 analysis by MALDI-MS. In our buffer system, ferulic acid produces more intense, consistently sharp mass spectra than 3,5-dihydroxybenzoic acid and sinapinic acid matrixes that are also generally useful for proteins of this size. Samples were collected immediately from the quench–flow apparatus, vortexed, mixed with ferulic acid matrix solution, and spotted onto the MALDI probe. The matrix mixture for these reactions contained 10 mg/mL ferulic acid in 2:1 ddH₂O/acetonitrile. After mixing 1 μ L of the reaction mixture with 9 μ L of matrix solution, a 1- μ L aliquot was deposited onto the MALDI sample probe. MALDI-TOFMS analysis was conducted with a linear time-of-flight instrument equipped with delayed extraction as described previously.³³ Under our experimental conditions, this instrument has a resolving power of about 1200 for $[\text{Stp1} + \text{H}]^+$ ions (17 391.8 Da). All spectra are summations of 100 individual laser shots. For statistical purposes, spectra of all MALDI samples were acquired in triplicate. Peak areas of Stp1 (E) and its phosphoenzyme intermediate (EP) were measured by summing the intensity under each peak following a linear baseline subtraction. Raw data were keyed directly into a spreadsheet for further calculation. The relative concentration of EP in each sample ($[\text{EP}]/[\text{E}]_0$) was calculated as the peak area of EP divided by the sum of EP and E peak areas. Because all time points were analyzed in triplicate, final EP concentrations used in the kinetic analysis represented the average of three measurements with error bars determined by their standard deviations. Relative EP concentration was plotted versus reaction time, and a nonlinear regression was used to fit the resulting curve to eq 5:

(32) Bender, M. L.; Kézdy, F. J.; Wedler, F. C. *J. Chem. Educ.* **1967**, *44*, 84–88.

(33) Christian, N. P.; Colby, S. M.; Giver, L.; Houston, C. T.; Arnold, R. J.; Ellington, A. D.; Reilly, J. P. *Rapid Commun. Mass Spectrom.* **1995**, *9*, 1061–1066.

(31) Lanzetta, P. A.; Alvarez, L. J.; Reinach, P. S.; Candia, O. A. *Anal. Biochem.* **1979**, *100*, 95–97.

$$\frac{[\text{EP}]}{[\text{E}]_0} = C(1 - e^{-bt}) \quad (5)$$

In eq 5, t is the duration of the reaction in seconds as established by the quench-flow instrument. The constants b and C contain the rate constants of interest, k_2 and k_3 (see Figure 1), and are defined by eqs 4 and 6, respectively.³² Note that C represents the relative concentration of EP that accumulates in the steady state.

$$C = \frac{\frac{k_2}{(k_2 + k_3)}}{1 + \left(\frac{K_m}{[S]_0}\right)} \quad (6)$$

K_m is the Michaelis constant, measured separately in the steady state, and $[S]_0$ is the initial substrate concentration. To ensure that the substrate was present at saturating concentrations, $[S]_0$ was chosen to be at least 10-fold higher than K_m for each substrate (within solubility limits). Furthermore, use of a high $[S]_0$ allows us to assume that this value remains virtually constant over the time scale of the reaction studied.

High-Performance Liquid Chromatography. Identification of oxidized enzyme in our Stp1 stock solution was facilitated by chromatographic separation of native from oxidized Stp1 using a Dionex GPM-2 HPLC system. 390 μM enzyme was injected onto a Vydac C₄ 330 Å 4.6 mm \times 250 mm column (cat no. 214TP54) in 20- μL aliquots. A gradient was run from 5 to 95% acetonitrile in 0.1% TFA (aq) over 90 min with a flow rate of 1 mL/min. The UV absorbance detector was set for 214 nm. Fractions were collected in 1.5-mL Eppendorf tubes and concentrated by lyophilization. Stp1 fractions were reconstituted in 50 μL of ddH₂O for peptide mapping.

Peptide Mapping of Stp1. One-microliter of TPCK-trypsin (1 mg/mL in 100 mM ammonium bicarbonate) and 49 μL of 100 mM ammonium bicarbonate buffer were added to each HPLC fraction from the Stp1 mixture. Digestion proceeded for 4 h at 37 °C. Reactions were quenched with 1 μL of neat TFA. Digest samples were prepared for MALDI analysis by mixing 1 part digestion mixture with 9 parts α -cyano-4-hydroxycinnamic acid solution (10 mg/mL in 2:1 acetonitrile/0.1% TFA). Spectra were calibrated externally with a mixture of bradykinin, melittin, bovine insulin chain A and chain B.

RESULTS AND DISCUSSION

Direct Observation of Phosphoenzyme Intermediates in the Steady State. A crucial step in this experiment is the trapping and detection of the EP intermediate. The former is accomplished by acidification of the reaction mixture with ferulic acid in ethanol containing 1% (v/v) TFA such that the final volume of TFA in the mixture is 0.3% (v/v). When the pH of the reaction volume is rapidly lowered, the enzyme denatures. Denaturing not only prevents it from binding additional substrate, but EP is no longer activated for hydrolysis following loss of the tertiary structure of the Stp1 binding pocket.¹⁴ All solutions in these preliminary experiments were mixed by hand. Because we expect the reaction to reach steady state within tens of milliseconds, trapped EP observed in this manner represents its steady-state concentration.

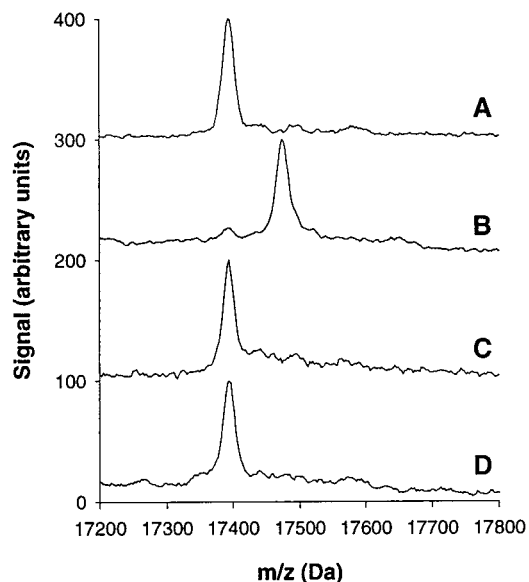


Figure 3. MALDI spectra summarizing steady-state experiments with *p*-NPP substrate. Steady-state trapping of EP is depicted in (B) as a 79.1 ± 1.6 Da mass shift relative to unphosphorylated Stp1 (A). Control experiments included mixing 3 mM K₂HPO₄ with Stp1 (C) and quenching the enzyme prior to adding *p*-NPP substrate (D). In both cases, no mass adducts are observed, suggesting that the EP species observed in (B) truly results from a catalytic process.

Figure 3 summarizes the steady-state trapping experiments on Stp1. Figure 3A is a MALDI spectrum of Stp1 acquired without substrate present. Trapping of EP is shown in Figure 3B, using 300 μM *p*-NPP as described previously. The enzyme increases in mass by 79.1 ± 1.6 Da, as externally calibrated from the parent ions of Stp1 and equine myoglobin ($[M + H]^+ = 16\,951.6$ Da). Notice that the enzyme is not 100% converted to EP, as a small ion signal corresponding to unphosphorylated Stp1 is still present. Figure 3C is a spectrum of Stp1 mixed with 3 mM K₂HPO₄. There is no evidence of an adduct species at 98 Da, eliminating the possibility that noncovalent attachment of PO₄H₃ can occur to any significant extent. Finally, the spectrum in Figure 3D was acquired using the same reaction mixture as that in Figure 3B. This time, however, the enzyme was mixed with quenching agent prior to substrate addition. This demonstrates that the denatured enzyme does not retain any significant activity. Therefore, the mass shift in Figure 3B corresponds to a trapped phosphoenzyme intermediate formed during the catalytic dephosphorylation of substrate.

The optimum concentration of TFA for quenching was determined by varying the TFA content of the ferulic acid solution introduced. Sufficient quenching agent must be added to denature the enzyme rapidly. Otherwise, some EP moieties hydrolyze before complete denaturation. For example, when an Stp1 reaction in the steady state was quenched by adding 0.1% (v/v) TFA, $[\text{EP}]/[\text{E}]_0$ was approximately 50%. $[\text{EP}]/[\text{E}]_0$ increased with TFA content until a limiting value was reached upon addition of 0.2% (v/v) TFA. For the experiments in Figure 3, we added 0.3% TFA to ensure efficient EP trapping. Similar optimization experiments were performed when we switched to the dimethylglutarate buffer system with a dichloroacetic acid (DCA) quench for the pre-steady-state kinetic studies.

Stp1 binds both aryl and alkyl phosphates as substrates, but catalyzes dephosphorylation of aryl phosphates more efficiently.¹⁰

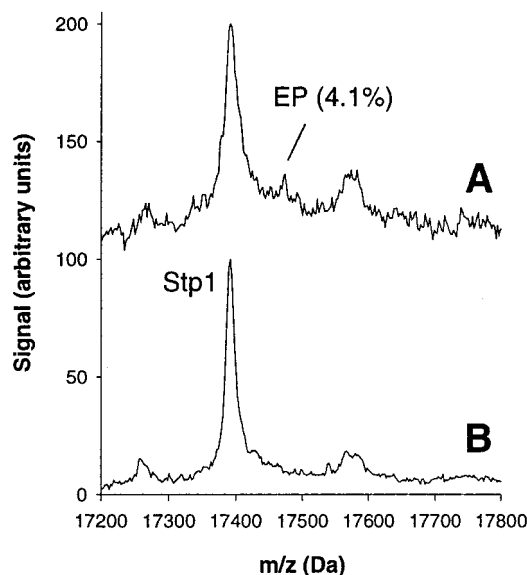


Figure 4. MALDI mass spectrum of Stp1 quenched during steady-state turnover of trifluoroethyl phosphate (A). Because this is a poor substrate for the enzyme, EP hydrolysis (k_3) is no longer rate limiting and only ~4% EP is observed in the steady state. A spectrum of Stp1 without substrate added is provided for comparison in (B).

An example of a poor enzyme substrate is presented in Figure 4A. 60 μM Stp1 was treated with 75 mM trifluoroethyl phosphate. Because in this case EP hydrolysis is not rate limiting, only about 4% EP is present in the steady state.

Although our purpose in this work is to obtain kinetic information, the direct observation of the EP intermediate is, itself, noteworthy. When deciphering an enzyme mechanism, formation of a covalent intermediate implies a double-displacement mechanism as shown in Figure 1. This is in contrast to a single-displacement scheme where the enzyme activates a water molecule for direct hydrolysis of substrate.¹³ EP has also been observed directly by other methods. For example, Guan and Dixon trapped EP while using ^{32}P -labeled substrate. When they ran a quenched reaction mixture on a denaturing gel, they noted that the radioactivity migrated with the protein band.³⁴ Anderson's group used ^{31}P NMR to detect the formation of a covalent phosphocysteine moiety during the reaction of a PTPase with a phosphorylated peptide.³⁵ Our method of observing EP does not require ^{32}P -enriched substrate and can be accomplished within minutes. Although phosphopeptides and proteins have been detected by MALDI before,^{2,3} the present experiment is unique in that the phosphorylated enzyme is a transient species that must be trapped in order to be observed.

Pre-Steady-State Kinetics. To validate the use of MALDI-TOF as a detector for pre-steady-state kinetics, our first samples were run in parallel with UV-visible absorption spectroscopy using *p*-NPP as the substrate. Typical MALDI data acquired from such time courses are presented in Figure 5. Relative EP concentrations ($[\text{EP}]/[\text{E}]_0$) were measured for samples acquired in triplicate. On the basis of the standard deviations of these measurements, the precision of the method is 1.9% $[\text{EP}]/[\text{E}]_0$.

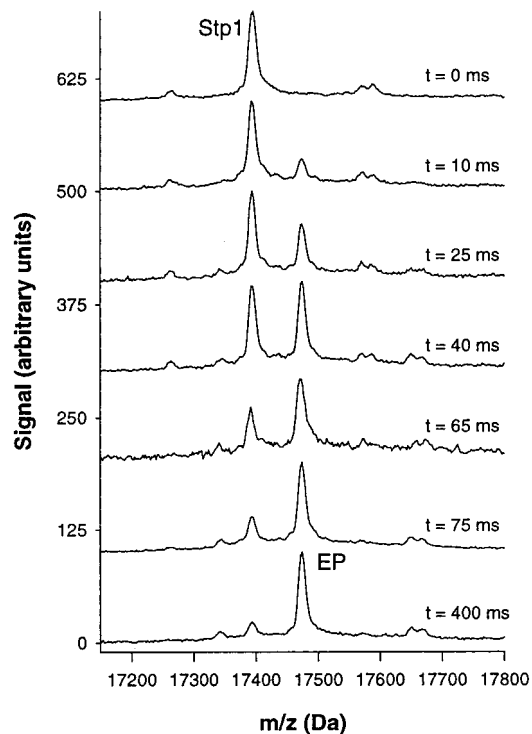


Figure 5. MALDI-TOF mass spectra acquired at various timepoints during the turnover of *p*-NPP by Stp1. The low-intensity peaks that appear between 17 550 and 17 700 Da correspond to ferulic acid matrix adducts with Stp1 and EP. Weaker peaks appearing at a lower mass than that of Stp1 correspond to the presence of post-translationally modified enzyme.

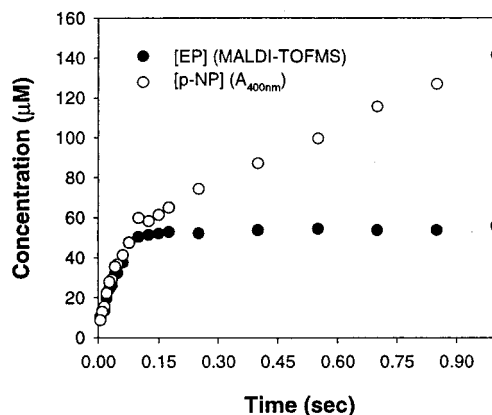


Figure 6. Representative data comparing [EP] acquired by MALDI (closed circles) versus [*p*-nitrophenol] measured spectrophotometrically at 400 nm (open circles). Relative EP concentrations obtained by MALDI were converted to absolute concentration by multiplying the data set by 60 μM . These data were drawn from experiment no. 4 in Table 2.

Best quantitation is obtained in the range of $[\text{EP}]/[\text{E}]_0$ from 10 to 90%, although some measurements were made down to 5%. Below this value, choosing integration limits becomes difficult as the peak height of EP is on the same order as baseline noise.

Because the MALDI and spectrophotometric methods measure EP and phenol release, respectively, the graphs of product concentration versus time have fundamentally dissimilar appearances as predicted by eqs 1 and 5. Figure 6 explicitly demonstrates the difference in concentration profiles between EP and *p*-nitrophenol as a function of time. Data for this figure were

(34) Guan, K. L.; Dixon, J. E. *J. Biol. Chem.* **1991**, *266*, 17026–17030.

(35) Cho, H.; Krishnaraj, R.; Kitas, E.; Bannwarth, W.; Walsh, C. T.; Anderson, K. S. *J. Am. Chem. Soc.* **1992**, *114*, 7296–7298.

Table 1. Measured Rate Constants for Substrates

substrate	K_m	$[S]_0$	pK_a^a	k_2 (s^{-1})	k_3 (s^{-1})
<i>p</i> -nitrophenyl phosphate (<i>p</i> -NPP)	150 μ M	3.0 mM	7.14	ND ^b	ND
<i>p</i> -fluorophenyl phosphate (<i>p</i> -FPP)	750 μ M	15 mM	9.9	29.2 \pm 3.8	1.89 \pm 0.46
phenyl phosphate (PP)	1050 μ M	15.7 mM	10.09	17.7 \pm 0.9	1.85 \pm 0.15
<i>p</i> -methylphenyl phosphate (<i>p</i> -MePP)	1150 μ M	11.5 mM	10.35	12.7 \pm 0.6	1.64 \pm 0.15
3,4-dimethylphenyl phosphate (3,4-DMPP)	1570 μ M	15.7 mM	10.42	11.8 \pm 0.6	1.73 \pm 0.16

^a The pK_a of the leaving group phenol. Values from ref 37. ^b ND, not determined.

acquired from the same set of rapidly quenched samples. MALDI $[EP]/[E]_0$ data were converted to an absolute concentration scale following multiplication by an enzyme concentration of 60 μ M. The rapid rise seen at early times in each trace describes the burst resulting from the double-displacement mechanism shown in Figure 1 when $k_2 > k_3$. Although the burst regions of the curves overlay reasonably well, they diverge once the reaction reaches the steady state. At this point, $[EP]$ remains constant and *p*-nitrophenol continues to be formed (though at a lower rate than in the pre-steady state).

Thus, validation of the MALDI-TOFMS kinetic assay cannot be accomplished by a simple overlay with spectrophotometric data. It seems logical that k_2 and k_3 could be extracted from each data set and compared directly. However, at this point we encounter a fundamental limitation in pre-steady-state kinetics.³⁶ As k_2 increases relative to k_3 , the pre-steady-state burst becomes steeper and the steady-state concentration of EP increases. When k_2 continues to increase, the differences between progress curves become increasingly subtle. Above a certain critical k_2/k_3 ratio, random error in experimental data prevents these subtleties from being distinguished by curve fitting, making it difficult or impossible to derive accurate rate constants from the progress curves.³⁶ In our experimental system, this critical value is approximately 100. We stress that this limitation exists as a result of the errors present in *all* experimental methods; it is not a failing of the MALDI-TOF methodology employed herein, as the spectrophotometric assay is also susceptible. Because of its high k_2 , rate constants measured for *p*-NPP had relative standard deviations in excess of 100%. Similar problems undoubtedly plagued Zechel et al., leading to their inability to extract absolute rate constants from their data.⁹ A thorough treatment of this phenomenon is given in a separate publication.³⁶

Despite this limitation, we can still determine if the progress curve derived by MALDI is consistent with the spectrophotometric analysis of *p*-NPP. The shape of the progress curve derived from MALDI data is determined by the coefficients b and C in eq 5. Curve fitting of the spectrophotometric data to eq 1 yields values for b and B without concern for the subtleties required to distinguish k_2 and k_3 . Values for $[S]_0$ and K_m for *p*-NPP are given in Table 1. With the aid of eq 7, we can transform the spectrophotometric data to represent $[EP]/[E]_0$ as a function of time, thus predicting how the MALDI data should appear.

$$C = \sqrt{\frac{B}{[E]_0}} \quad (7)$$

Figure 7 is an example of how experimental MALDI data overlays a prediction derived from spectrophotometric analysis of the same samples. A comparison of b and C values for several replicate runs with *p*-NPP is given in Table 2. Clearly, the MALDI and spectrophotometric data are consistent. Furthermore, note that the MALDI data are randomly distributed about the recalculated spectrophotometric data. This is particularly apparent in the steady-state portion of Figure 7. If EP experienced the sort of ionization bias that has been reported for small phosphopeptides,^{2,3} we would expect the relative EP concentration from MALDI data to be systematically low. Therefore, we conclude that the attachment of phosphate to an enzyme as large as Stp1 does not perturb its ionization efficiency to a significant extent.

Substrate Effects on Catalysis. The capability of studying nonchromophoric substrates enables us to investigate a series of substrates by quench–flow MALDI-TOFMS. Our goal is to measure the effect of substrate on the rate of EP formation (k_2). As demonstrated by Figure 1, the leaving group oxygen bears a partial negative charge during P–O bond scission. If we stabilize this charge by the addition of electron-withdrawing ring substituents, the reaction speeds up. Therefore, we expect to observe a corresponding enhancement in k_2 as electron-withdrawing substituents are added.

Results obtained with a few substrates, along with the corresponding $[S]_0$ and experimentally determined K_m values, are listed in Table 1. Values for k_2 and k_3 were obtained by fitting MALDI-generated progress curves to eq 5. Each substrate was analyzed by three separate runs through the quench–flow instrument. Rate constants and their errors were obtained by averaging the sets of rate constants from all three runs of the same substrate and computing the standard deviation.

As mentioned above, relative standard deviations for *p*-NPP were over 100%. This is indicative of a system with a k_2/k_3 ratio that is too high for reliable curve fitting.³⁶ On the other hand, k_2 values for the substrates presented here are all within the range that can be analyzed reliably by pre-steady-state methods. As a result, the precision of our measurements is greatly improved compared with that of the *p*-NPP experiment. The relative standard deviations of all k_2 values are under 5% except for that of *p*-FPP (13.0%). Because k_3 corresponds to hydrolysis of EP, we do not expect it to vary with substrate. In fact, k_3 values are quite consistent for all substrates examined.

Figure 8 is an overlay of the progress curves from the four substrates studied and explicitly demonstrates the trend that appears in the data as k_2 becomes larger than k_3 . If one

(36) Taylor, W. P.; Houston, C. T.; Zhang, Z.-Y.; Reilly, J. P.; Widlanski, T. S., manuscript in preparation.

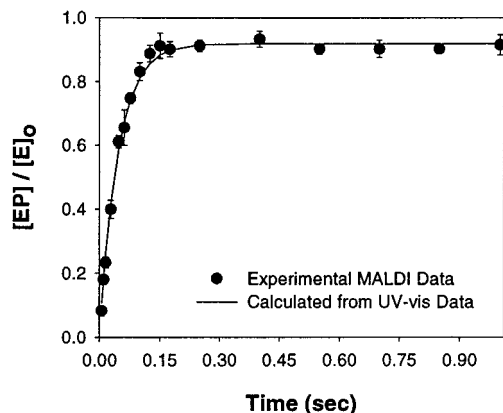


Figure 7. Comparison of reaction progress curves for EP measured by MALDI (closed circles) with that predicted by parallel absorbance measurements of *p*-nitrophenol at 400 nm (line). Error bars represent the standard deviation of three runs for each time point. This plot demonstrates typical data obtained for a single experiment (experiment no. 2 from Table 2).

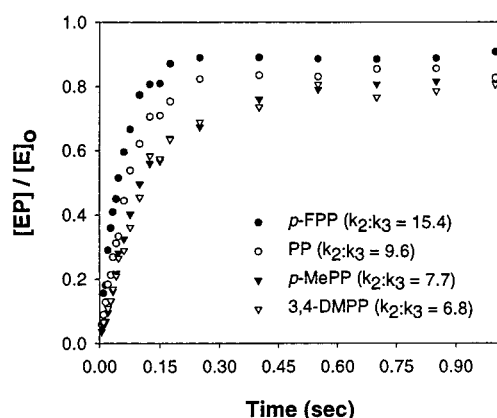


Figure 8. Overlay of progress curves for *p*-fluorophenyl phosphate (*p*-FPP), phenyl phosphate (PP), *p*-methylphenyl phosphate (*p*-MePP), and 3,4-dimethylphenyl phosphate (3,4-DMPP). Note that as the ratio of k_2 to k_3 increases, the shape of each curve changes such that the pre-steady-state burst is steeper and the steady-state conversion of Stp1 to EP is higher.

extrapolates the trend observed in this figure, it is not surprising that the differences between the curves become increasingly subtle for higher values of k_2/k_3 .

Our prediction that stabilization of the leaving group phenoxide should increase k_2 is demonstrated experimentally by the Brønsted plot in Figure 9. By plotting the log of k_2 versus the pK_a of the leaving-group phenol, we can quantify the stability of the phenoxide species formed by PTPase-catalyzed hydrolysis of each substrate listed in Table 1.

Finally, although we demonstrate a limitation of pre-steady-state kinetics for substrates with low pK_a values (such as *p*-NPP),³⁶ it is noteworthy that the hydroxyl of tyrosine has a pK_a in the range of 10.0–10.3.³⁸ As indicated by the Brønsted plot in Figure 10, we are able to obtain reliable pre-steady-state data for substrates in this pK_a range. Thus, although pre-steady-state kinetic methods may not be successful for artificial substrates with

Table 2. Comparison of Curve-Fit Coefficients from *p*-NPP Progress Curves

expt.	b_{MALDI}^a	b_{A400}^b	% diff. in b	C_{MALDI}^a	C_{A400}^c	% diff. in C
1	23.4	28.2	17.0	0.918	0.903	1.7
2	21.5	26.8	19.8	0.921	0.909	1.4
3	18.4	24.0	23.5	0.907	0.929	2.4
4	21.4	22.6	5.5	0.906	0.921	1.6

^a Obtained from curve fit to eq 5. ^b Obtained from curve fit to eq 1. ^c Calculated from B per eq 7.

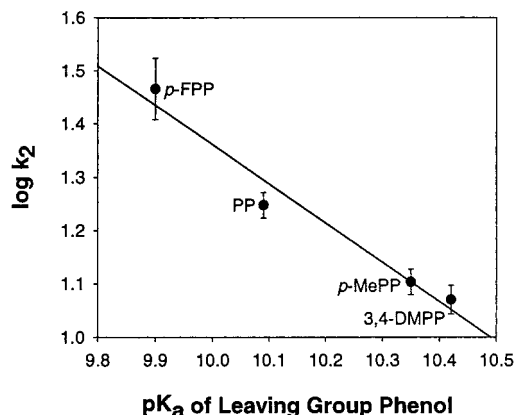


Figure 9. Brønsted plot demonstrating the dependence of k_2 on the pK_a of the leaving group. As the pK_a decreases, the stability of the phenolate anion leaving group is improved such that k_2 proceeds more favorably.

strongly electron-withdrawing substituents, they should be quite compatible with biochemically relevant protein and peptidal substrates.

Identification of Enzyme Heterogeneities. Because clean resolution of the enzyme and EP signals in the mass spectra is crucial for reliable peak integration, any sample heterogeneity that causes peak broadening is problematic. As our original stock solution of enzyme aged, Stp1 began to exhibit high mass tailing in the mass spectrum. HPLC separation on a C_4 column revealed that there were at least four protein components present in the sample. The dominant peak in the chromatogram (fraction 3) corresponded to intact, unmodified Stp1. MALDI spectra acquired from fraction 3 were very sharp and symmetric. Tryptic digestion of all four fractions revealed oxidation to be the source of the high mass tailing. Figure 10 contains a portion of the peptide maps generated from each HPLC fraction of the Stp1 sample. Note that peptides T3 and T13 appear as doublets in fractions 1, 2, and 4. These doublets are separated by 16 Da. T3 and T13 each contain one of four methionine residues present in the protein that can be oxidized to sulfoxide moieties. We conclude from this analysis that a population of oxidized enzyme was present in the sample. Because the individual oxidation products were not resolvable in MALDI-TOF spectra of the intact enzyme, the modification manifested itself as tailing toward high mass. Subsequent kinetics studies were conducted with newer batches of unoxidized Stp1. This ability to detect and identify such enzyme modifications is another clear advantage of mass spectrometric detection over spectrophotometry. In a standard spectrophotometric experiment, enzyme modification of any sort would not be evident. Because

(37) Sejeant, E.; Dempsey, B. *Ionisation Constants of Organic Acids in Aqueous Solution*, Pergamon Press: Elmsford, NY, 1979.

(38) Creighton, T. E. *Proteins*, 2nd ed.; Freeman: New York, 1993; p 4.

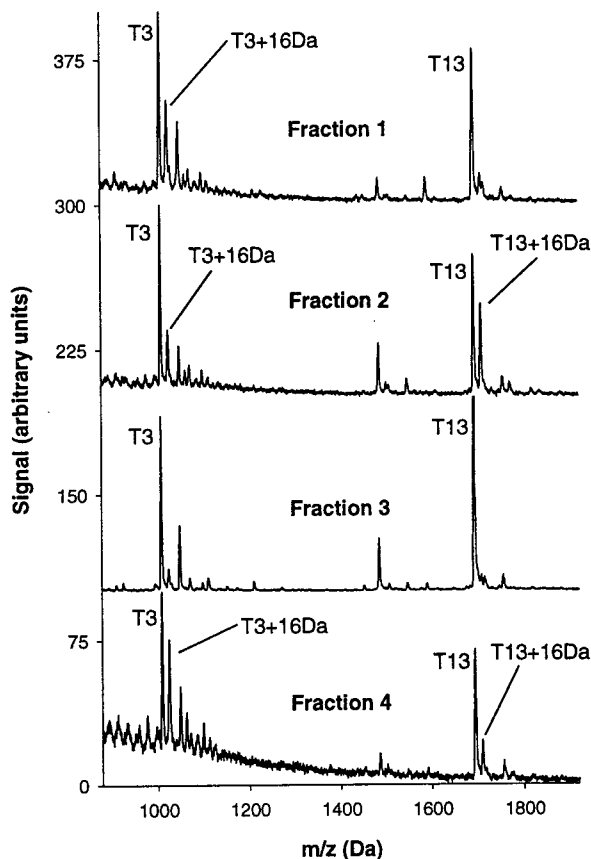


Figure 10. MALDI-TOF mass spectra of tryptic digestions of Stp1 HPLC fractions. Fractions 1, 2, and 4 contain oxidized protein as demonstrated by the +16 Da adducts on peptides T3 and T13. Fraction 3 contained native enzyme.

initial enzyme concentration is an important parameter in the analysis (eqs 2 and 3), alteration of enzyme activity owing to modification of any sort would artificially skew the rate constants derived from the experiment.

Post-translational modification is another example of enzyme heterogeneity encountered in this experiment. As noted in Figure 5, a low mass peak appears in some of our Stp1 spectra at $[M + H]^+ = 17\,261.5 \pm 1.3$ Da, 130 Da lower in mass than Stp1. Although barely evident in Figure 5, other data reveal that the lower-mass protein in the mixture has the same activity as Stp1,

as indicated by the 80-Da shift observed in the presence of substrate. This lighter protein component comprises ~5% of the total protein in the sample and appears to be Stp1 following a loss of its N-terminal methionine residue. It is very likely that the activity of this post-translationally modified Stp1 is the same as that of its native precursor. However, this may not be true of all post-translational modifications. Spectrophotometric assays that study only product release would obtain data that contains contributions from both species present in the mixture. The MALDI-TOF method, however, effectively decouples the modified and native enzymes such that data are collected only for the native enzyme. In principle, we could compare the kinetics derived from the native and modified enzymes to see if they differ. However, the amount of modified protein in this particular study is too low for reliable peak integration.

CONCLUSIONS

MALDI-TOFMS can readily be coupled off-line with quench-flow techniques to measure pre-steady-state kinetics. As described in this work, mass spectrometry holds several advantages over spectrophotometric detection. We stress that this method is not exclusive to phosphatases; it should work for any enzyme that obeys the kinetic scheme shown in Figure 1.^{7,9}

The advantages of mass spectrometric detection in kinetics experiments described in this paper are applicable to those of electrospray ionization as well as of MALDI. Although electrospray ionization instruments have an advantage in that they are more easily interfaced with rapid quench methods, they are also more easily fouled and their spectra more readily perturbed by the presence of buffers and other sample additives than MALDI is.³⁹⁻⁴¹ Proper buffering is essential for maintaining the enzyme in a native and active state. Thus, the availability of MALDI as an alternative ionization technique gives the enzymologist greater freedom in choosing an experimental system that is compatible with the technology used to probe it.

ACKNOWLEDGMENT

The authors are grateful to Stephen Antonelli for synthesizing the aryl phosphate substrates used in this study. We also thank Z.-Y. Zhang for the preliminary samples of Stp1 and a plasmid encoding this protein. This work was supported by the National Science Foundation and the National Institutes of Health.

(39) Chait, B. T.; Kent, S. B. *Science (Washington, D.C.)* **1993**, *257*, 1885-1893.

(40) Beavis, R. C.; Chait, B. T. *Anal. Chem.* **1990**, *62*, 1836-1840.

(41) Strupat, K.; Karas, M.; Hillenkamp, F. *Int. J. Mass Spectrom. Ion Processes* **1991**, *111*, 89-102.

Received for review December 30, 1999. Accepted April 12, 2000.

AC991499M